Fast evaluation of central moments for non-Gaussian random loads in vibration fatigue

M. Palmieri[1*], J. Slavič[2], F, Cianetti[1]

[1] *University of Perugia, Department of Engineering, Via G. Duranti 93, 06125 Perugia, Italy*

[2] *University of Ljubljana, Faculty of Mechanical Engineering, Aškerčeva cesta 6, 1000, Ljubljana, Slovenia*

Cite as:
M. Palmieri,J. Slavič, F, Cianetti, Mechanical Systems and Signal Processing, Volume 228, 1 April 2025, 112434`https://doi.org/10.1016/j.ymssp.2025.112434`

Abstract

In vibration fatigue analysis, spectral methods are used to evaluate the fatigue damage of structures experiencing random vibrations. Spectral methods fail under non-Gaussian and non-stationary loading conditions and various solutions have been proposed. Correction coefficients are promising and depend on the kurtosis and skewness of the system's response, which requires extensive time-domain analyses. Performing time-domain analysis undermines the computational efficiency of spectral methods. The present manuscript proposes a modal decomposition-based approach to numerically efficiently compute the central moments required to obtain the kurtosis and skewness. The proposed method is numerically validated on a structure subjected to non-Gaussian random loads. The proposed method demonstrates results identical to the standard approach, showing a reduction in computation time of around two orders of magnitude. This extends the applicability

*Corresponding author
Tel: +39 075 585 3728
Email address: massimiliano.palmieri@unipg.it (M. Palmieri)

of spectral methods in conjunction with correction coefficients for numerical estimation of fatigue damage in the frequency domain even in the case of non-Gaussian loadings.

Keywords: Vibration fatigue, Spectral methods, non-Gaussian loads, Modal decomposition

---

1. Introduction

Fatigue damage is a critical concern for structures subjected to random vibrations, especially in engineering applications where reliability and longevity are paramount. The traditional approach in vibration fatigue to address the fatigue damage is the time domain approach [1] thanks to which it is possible to simulate mechanical systems showing both linear and non-linear behavior and subjected to any loads from deterministic to random, even if non-stationary or non-Gaussian. Despite the time-domain approach being considered the reference in vibration fatigue, it is a time-consuming approach. Indeed, for each element of the model, it is necessary to evaluate the stress tensor, reducing it with a multi-axial criterion, and extract the fatigue cycles by a cycle-counting algorithm aimed to evaluate the fatigue damage [2]. To reduce the computational effort, in recent years, the fatigue damage induced by mechanical vibrations is generally addressed by frequency-domain methods [3]. Several techniques have been developed for different types of excitation such as Sine-Sweep excitation [4] and Sine-on-Random loadings [5], but due to their extensive application, most of the effort is allocated to random vibrations [6]. Frequency domain methods, applied to random loads, base the calculation on a spectral representation of the random process through the Power Spectral Density (PSD) [7] that entirely and completely represents the random process if it is stationary and Gaussian. Under such a hypothesis, spectral methods offer a streamlined pathway to predict fatigue life with shortened computational time compared to standard time-domain procedures.

Real-world operating conditions however do not always conform with the hypothesis of stationary and Gaussian stress processes. The non-Gaussian and non-stationary stress state of a component is due to the nature of the applied loads, which may be inherently non-Gaussian, such as road roughness [8], pressure fluctuations [9], sea waves [10] or may result from non-linearities (e.g. contact, end-strokes, non-linear spring-damper) of the system [11].

Whichever the source of the non-Gaussian stress response, if they occur, the conventional spectral methods, developed for high-cycle fatigue conditions, fail to provide a true representation of the damage experienced by the structure. Palmieri et al. [12] compared the experimental and numerical-obtained fatigue life of laboratory structures experiencing non-Gaussian and non-stationary loads demonstrating how spectral methods can fail in case of non-normal loads. Cianetti et al. [13] and Wang et al. [14] numerically demonstrated the committed error deriving by the use of spectral methods in the case of non-Gaussian loads. The discrepancy in the estimation of fatigue life by using spectral methods arises because non-Gaussian characteristics such as kurtosis and skewness of the stress response are not inherently captured in the spectral domain.

To overcome this limitation, the engineering community is widely active in developing various techniques to address this issue. For example, in 2015 and 2017 respectively, Ding et al. [9] and Chang et al. [15] modified the Dirlik and Tovo-Benasciutti distribution by a Hermite transformation to account for the non-Gaussian nature of random stress. Of interest are the approaches proposed by Wolfsteiner [16] and the one proposed in 2020 by Trapp et al. [17] based on the decomposition of non-Gaussian process into several segments of underlying Gaussian process to compute the fatigue damage with standard Gaussian-based spectral methods. In the context of product design, the most promising approaches to adopt when non-Gaussian stress occurs, are those based on correction factor. This is due to all of them being of practical implementation and easy-to-use perfectly fulfill with design process [12]. These factors adjust the fatigue damage computed via spectral methods to better align with the non-Gaussian nature of the stress process. The most known correction coefficients were proposed by Winterstein et al. [18], Wang et al. [19] and Braccesi et al. [20]. In 2017, Cianetti et al. [21] proposed a new formulation of Braccesi's coefficient to account for strongly non-Gaussian and zero-skewed time series. In 2023, Yuan et al. [22] proposed the weighting factor based on the bandwidth parameters, slope parameter of the S–N curve, and skewness and kurtosis of non-Gaussian processes to account for non-Gaussianity of a wide-band random process. Despite their effectiveness, the practical implementation of correction factors still requires the knowledge of higher-order central moments of the stress response for each element of the structure. As demonstrated by Khim et al. [23], by Sgamma et al. [24], by Braccesi et al. [25] and by Trapp et al. [26], the response of the system varies according to the dynamic behavior of the structures and according to

the nature of the excitation. Due to this, time-domain simulations are the only possible path to derive kurtosis and skewness of the structural response. With time-domain analysis, however, the key advantage of spectral methods (the computational efficiency) is lost.

To intensify the use of spectral methods in conjunction with correction coefficient approaches, it is fundamental to derive an approach aimed at quickly assessing the statistical parameters of the system's response. To this aim, this research introduces a fast method, still in the time domain, designed to calculate central moments, thus also kurtosis and skewness, with significantly reduced computational effort. The proposed method is based on modal analysis [27, 28, 29]. By first computing the statistical moments of the modal coordinates, it is possible, through a combination with the modal shapes, to obtain the central moments of the physical response without the need to evaluate the latter for each element. The approach proposed herein is similar to that of Bracessi et al. [30], which computes the spectral moments directly from the PSD matrix of modal coordinates. This proposed approach circumvents the intensive computational demands traditionally associated with evaluating the structural response and allows for the rapid calculation of the correction coefficient. Thus, the fatigue damage under non-Gaussian events, can be efficiently computed in the frequency domain adjusting the fatigue damage with correction coefficient methods.

The efficacy of the proposed method is demonstrated through its application to a simple structure subjected to different stationary and non-stationary non-Gaussian loading conditions. The results, which are benchmarked against standard analyses, not only confirm the accuracy of the results but also highlight a substantial reduction in computational time. This study positions the integration of spectral methods with correction coefficients, supported by the proposed efficient time-domain calculation of the statistical moments, as a robust framework for addressing fatigue damage under non-Gaussian loading conditions. The enhanced efficiency and accuracy offered by this approach hold significant promise for its adoption in engineering practices where computational resources are a limiting factor.

The presented paper is organized as follows: Sec. 2 introduces a short theoretical background about signal properties, structural dynamics, and vibration fatigue, Sec. 3 illustrates the proposed method to rapidly compute the central moments of a structural response starting by the modal coordinates, Sec. 4 shows the test case used to evaluate the accuracy of the proposed method while Sec. 5 draws the conclusions.

2. Theoretical background

The present section outlines the fundamental principles for addressing vibration-fatigue phenomena. It highlights theoretical aspects such as signal processing (Sec. 2.1), structural dynamics and the modal approach (Sec. 2.2), spectral methods for fatigue damage calculation, and the corrective coefficient approach (Sec. 2.3).

2.1. Random process

A random process can be stationary or non-stationary, Gaussian or non-Gaussian [31]. A random variable x is said to be Gaussian if its probability density function $p(x)$ (PDF) is given by:

$$p(x) = \frac{1}{\sqrt{2\pi\sigma^2}} e^{-\frac{(x-\mu)^2}{2\sigma^2}}. \tag{1}$$

The Gaussian probability density function is entirely defined by the mean value μ and the variance σ^2 [7, 31]. The mean value μ and the variance are respectively the first and the second central statistical moments. A central moment is a statistical parameter that measures the deviation from the mean μ. The j^{-th} central statistical moment can be computed as follow [31]:

$$m_j = E\left[(x_i - E(x_i))^j\right], \tag{2}$$

where $E[\cdot]$ is the expected value operator and n is the number of points in the sample time history [31].
Random processes may not follow a Gaussian distribution. In this case, the first two central statistical moments are not sufficient to characterize the probability distribution [31]. To measure the deviation of a distribution with respect to a Gaussian one, two statistical descriptors, namely skewness s_k and kurtosis k_u, are used:

$$\begin{aligned} s_k &= \frac{m_3}{\sigma^3} = \frac{m_3}{(m_2)^{3/2}}, \\ k_u &= \frac{m_4}{\sigma^4} = \frac{m_4}{(m_2)^2}. \end{aligned} \tag{3}$$

These are the higher-order statistical moments and are the third and fourth-order statistical moments normalized with respect to the standard deviation.

A Gaussian process has the kurtosis $k_u = 3$ and the skewness $s_k = 0$. The skewness s_k is a measure of the asymmetry of the PDF while the kurtosis k_u characterizes the sharpness of the PDF peak and the width of the PDF tails. This means that kurtosis identifies extreme events in the random process and significantly affects the fatigue life.
If the random process is stationary and Gaussian, it can be completely defined in the frequency domain by the Power Spectral Density $S(f)$ where f denotes the frequency vector [6]. The Power Spectral Density describes how the power is distributed in the frequency domain. The two-side Power Spectral Density $S(f)$ is defined as the Fourier transform of the autocorrelation function:

$$S(f) = \int_{-\infty}^{\infty} R_{xx}(\tau) e^{-j2\pi f\tau} \mathrm{d}\tau, \tag{4}$$

where $R_{xx} = E\left[x(t) \cdot x(t+\tau)\right]$.
In vibration fatigue, the one-side PSD is however generally use and it is defined as:

$$G(f) = \begin{cases} 2S(f) & \text{if } f > 0, \\ S(f) & \text{if } f = 0, \\ 0 & \text{if } f < 0. \end{cases}$$

Both PSD, the two-side and the one-side, are further described by the spectral moments M_n. For the one-side PSD $G(f)$, the spectral moments can be computed as:

$$M_n = \int_0^{\infty} (2\pi f)^n \left|G(f)\right| \mathrm{d}f, \tag{5}$$

where n denotes the order of the spectral moment.
The zeroth order spectral moment, being the area under the PSD function G(f), coincides with variance (second statistical moment) of the time process $x(t)$, while M_2 and M_4 coincide with the variance of its derivatives, $\dot{x}(t)$ and $\ddot{x}(t)$ [32]. Particular combinations of spectral moments are related to signal characteristics, like the number of positive zero crossings, ν^+, the number of peaks for time unit ν_p and the irregularity factor γ [32]:

$$\begin{aligned} \nu^{+} &= \sqrt{\frac{M_2}{M_0}}\,, \\ \nu_p &= \sqrt{\frac{M_4}{M_2}}\,, \\ \gamma &= \frac{M_2}{\sqrt{M_0 M_4}}\,. \end{aligned} \tag{6}$$

Based on spectral moments, it is possible to understand the nature of the random process (narrow-band, wide-band) [32] and select the appropriate probability distribution of cycles amplitude to compute the fatigue damage (Sec. 2.3).

2.2. Structural dynamics

For a multi-degree of freedom system (mdof), the associated equation of motion can be defined as follow [32]:

$$[M]\,\{\ddot{x}\} + [C]\,\{\dot{x}\} + [K]\,\{x\} = \{f\}, \tag{7}$$

where $\{x\}$ represents the vector of degree of freedom and $\{f\}$ is the excitation force vector. $[M]$, $[C]$, and $[K]$ are the mass, damping, and stiffness matrix, respectively. The equations of motion shown in Eq. (7) are generally coupled and must be solved simultaneously to obtain the physical response of the system. If the component behaves like a Linear Time-Invariant (LTI) system, Eq. (7) can be re-written by introducing a change of variables from the physical coordinates $\{x\}$ to the modal coordinates $\{q\}$, using the relation:

$$\{x\} = [\phi]\{q(t)\}. \tag{8}$$

The transformation into modal space allows for a reduction in the number of dynamic equations, from the total number of degrees of freedom of the system to the number of selected vibrating modes [32]. The mass normalized equation of motion is:

$$[I]\,\{\ddot{q}\} + [2\xi\omega_0]\,\{\dot{q}\} + \left[\omega_0^2\right]\,\{q\} = [\phi]^T\,\{f\}, \tag{9}$$

where $[I]$ is the identity matrix, $[2\xi\omega_0]$ is the damping matrix, $[\omega_0^2]$ is the matrix of natural frequencies, and $[\phi]$ is the modal shapes matrix. Since the

matrices $[I]$, $[2\xi\omega_0]$, and $[\omega_0^2]$ are diagonal, each equation of Eq. (9) represents the equation of motion of a single degree of freedom system with unitary mass and can be solved independently from the others in terms of the modal coordinates $q(t)$.
There are several ways to obtain the modal coordinates $q(t)$: Firstly, the equation of motion in modal space (Eq. 9) can be integrated using numerical computing software. Another possibility is to extract the modal coordinates directly through Finite Element Analysis [33]. Alternatively, modal coordinates can be obtained via multibody analysis, where the component to be verified is modeled as a flexible body [34]. In the latter case, the system can also be non-linear and thus a source of non-Gaussian excitation. However, even in this scenario, since the flexible component is modeled using the modal approach, it is possible to derive the modal coordinates as an output. Once modal coordinates are known, the physical response of each element of the flexible component in the time domain can be obtained according to Eq. (8). The physical response $\{x\}$ takes the physical meaning of the scaling modal shapes. If, for example, the modal shapes $[\phi]$ are derived in terms of stress $[\phi^\sigma]$, then the stress time history is obtained by Eq. (8) [27].
Under the assumption of stationary and Gaussian excitations time histories, the fastest way to obtain the structural response of the component is to work in the frequency domain. Starting by Eq. (9), it is possible to derive the Frequency Response Function (FRF) matrix of modal coordinates, of dimension $(n \times n)$ where n is the number of considered vibrating modes [27]:

$$[H_q(\omega)] = \frac{[\phi]^T}{-[I]\,\omega^2 + [2\xi\omega_0]\,j\,\omega + [\omega_0^2]}. \tag{10}$$

Once the frequency response function $[H_q(\omega)]$ is known, the Power Spectral Density matrix of the physical response $[S_x(\omega)]$ can be computed according to [27]:

$$[G_x(\omega)] = [\phi^x] \cdot \Big[[H_q(\omega)]\,[G_F(\omega)]\,[H_q(\omega)]^T\Big] \cdot [\phi^x]^T, \tag{11}$$

where $[\phi^x]$ is the matrix of modal shapes of the chosen output derivable from a finite element model and $[S_F(\omega)]$ is the Power Spectral Density (PSD) matrix of the excitation force. Also in this case, the physical quantity of $[G_x(\omega)]$ depends on the modal shapes: if modal shapes derived by FEA analysis are expressed in terms of stress $[\phi^\sigma]$, then the output PSD would

be $[G_\sigma(\omega)]$ taking the dimension of stress^2/Hz. Relative to the stress PSD matrix, in case the analyzed set of elements is subjected to a multiaxial stress state, the matrix of Power Spectral Density $[S_\sigma(\omega)]$ must be reduced into an equivalent one. Although different methods are available in literature [35, 36, 37], the Pitoiset method [38] evaluates the equivalent uniaxial Von-Mises stress Power Spectral Density as:

$$G_\sigma^{eqv}(\omega) = \text{Trace}\left[[Q] \cdot [G_\sigma(\omega)]\right], \tag{12}$$

where the matrix $[Q]$ is a matrix of coefficients. Once $G_\sigma^{eqv}(\omega)$ is known, it is possible to evaluate the fatigue damage according to the method introduced in the next section.

2.3. Fatigue damage in frequency domain

Once the stress PSD $G_\sigma^{eqv}(\omega)$ is known, the fatigue damage in the frequency domain can be computed with the Palmgren-Miner rule [6]:

$$D_g = \nu_p \, C^{-1} \int_0^\infty s^k \, p(s) \, \mathrm{d}s, \tag{13}$$

where s represents the cycle amplitude, ν_p is the number of maxima per unit of time derivable from the spectral moments of the stress PSD $G_\sigma^{eqv}(\omega)$ and $p(s)$ is the cycle amplitude probability density function (PDF) of the stress cycles. k and C are the parameters describing the s-N curve of the material [6]:

$$C = s^k N, \tag{14}$$

where N is the number of cycles-to-failure and s represents the cycles amplitude. If the process is Gaussian and stationary, and considering a linear elastic behavior of the material, the fatigue damage computed in the frequency domain is very close to that derivable by a time domain analysis. The only challenge in Eq. (13) is to use an expression for the probability density function of stress peaks $p(s)$ that correctly represents the underlying process. Different probability density functions have been proposed in the literature according to properties of the random process (*i.g.* narrow-band, bi-model, wide-band) [6, 39].

Whichever spectral method is used, the PDF $p(s)$ of the stress cycles is always computed via the spectral moments. The spectral moments M_n can be obtained from the stress PSD of each element defined in Eq. 12 or, in a

faster manner, from the PSD matrix of modal coordinates [30]. Since spectral methods base the calculation of the fatigue damage on spectral moments (thus on the PSD), they are theoretically no longer applicable in case the structural response in the time domain is expected to be non-Gaussian [12]. The PSD is not able to capture the non-Gaussian properties of a time signal and thus, the estimated fatigue damage can result to be not accurate. Under the condition of high-cycle fatigue, a possible way to tackle this issue is by utilizing a correction factor [18–22]. This approach foresees to evaluate the fatigue damage D_{ng}, resulting from the non-Gaussian stress time history, by multiplying the Gaussian damage D_g (obtainable by Eq. (13) omitting the non-Gaussianity of the process) with a corrective non-Gaussianity factor λ_{ng} as:

$$D_{ng} = \lambda_{ng} \cdot D_g. \tag{15}$$

In the literature, there are four main correction coefficients. The first two polynomial relations were proposed by Winterstein $\lambda_{ng,W}$ [18] and Wang $\lambda_{ng,WG}$ [19] and are shown in (16) and in (17) respectively.

$$\lambda_{ng,W} = \left(\frac{\beta\sqrt{\pi}}{2\Gamma(1+|\nu|)}\right)^k \left(\frac{\Gamma(1+k|\nu|)}{\Gamma(1+k/2)}\right), \tag{16}$$

where:

$$\begin{aligned}
\beta &= \frac{1}{\sqrt{1+2h_3^3+6h_4^2}},\\
\nu &= \sqrt{\frac{4}{\pi}(1+h_2+h_4)-1},\\
h_1 &= \frac{s_k}{6},\\
h_2 &= \frac{k_u-3}{24},\\
h_3 &= \frac{s_k}{6(1+6h_4)},\\
h_4 &= \frac{\sqrt{1+1.5(k_u-3)}-1}{18}.
\end{aligned}$$

$$\lambda_{ng,WG} = \beta^m \left(1 + k(k-1)h_2 2 + k(k+1)\beta h_1 \frac{\sigma}{S_{ut}}\right). \tag{17}$$

In previous equations, k is the slope of the S-N curve while k_u and s_k are the kurtosis and the skewness of the stress response. In 2009 Braccesi et al. [20] proposed a new correction coefficient $\lambda_{ng,B}$ and in 2017 Cianetti et al. [21] proposed an upgrade version of the correction factor $\lambda_{ng,C}$ to account for strongly non-Gaussian stress response:

$$\lambda_{ng,B} = \exp\left(\frac{k^{3/2}}{\pi}\left(\frac{k_u - 3}{5} - \frac{s_k^2}{4}\right)\right). \tag{18}$$

$$\lambda_{ng,C} = \exp\left(\frac{k^{3/2}}{\pi(0.156 + 0.416k_u)}\left(\frac{k_u - 3}{5}\right)\right). \tag{19}$$

The calculation of the corrective coefficients requires the knowledge of the skewness and kurtosis values of the stress response of each element of the model. This, in turn, would require an analysis in the time domain aimed to evaluate the stress response and thus calculate the central statistical moments. This task however diminishes the computational advantages of spectral methods making these approaches not widely used.

3. Fast evaluation of central moments using the modal approach

In section 2, it was demonstrated that fatigue damage calculations in the frequency domain, using spectral methods for non-Gaussian responses, can be accurately addressed by applying correction coefficients that account for the non-Gaussian nature of the random processes. The effectiveness of these correction coefficients is supported by several studies [22], where the corrected fatigue life aligns well with results from experimental tests or time-domain numerical simulations [37, 40].
The correction factors presented from Eq. (16) to Eq. (19) are functions of the kurtosis (k_u) and skewness (s_k) of the structural response. However, these non-Gaussian parameters (k_u, s_k) can only be evaluated through the stress response in the time domain. Computing the stress response for each element in a finite element (FE) model requires significant computational time, which limits the practical use of correction factors. To enhance the applicability of these correction coefficients (λ_{ng}), it is crucial to develop a method that allows obtaining the central statistical moments both accurately and quickly. This challenge can be addressed using the modal approach (Section 2.2). Specifically, since the structural response of an element can be represented as a linear combination of modal coordinates and modal shapes as shown in

Eq. (8), then also the statistical central moments of the structural response can be derived directly from the statistical central moments of the modal coordinates. Since the number of equations of motion formulated in modal space is significantly smaller than those in physical space, the modal approach can likewise be employed to calculate the central moments from the modal coordinates accurately and efficiently.
To illustrate the proposed approach, let us first consider a random process Z, which is the sum of two random variables X and Y.

$$Z = aX + bY\,, \tag{20}$$

where a and b are constant terms. Eq. (20) can be assimilated to the modal response of a two degree of freedom system: X and Y make a match with the modal coordinates q_1 and q_2 respectively while a and b pair up with the modal shapes $\phi_{i,1}$ and $\phi_{i,2}$ respectively (Eq. 8).
To estimate the second order statistical moments of random variable Z, it is possible to substitute Eq. (20) into Eq. (2):

$$\begin{aligned} m_2(Z) = E\left[(Z-\mu_Z)^2\right] = E[a^2(X-\mu_X)^2 + b^2(Y-\mu_y)^2 + \\ + 2\,a\,b\,(X-\mu_X)(Y-\mu_Y)]\,. \end{aligned} \tag{21}$$

Due to the linearity of expectation [31], the expected values can be computed separately and the constant terms can be moved out of the expectation without error. Thus, Eq. (21) can be further rewritten as:

$$\begin{aligned} m_2(Z) = a^2\,E[(X-\mu_X)^2] + b^2\,E[(Y-\mu_y)^2] + \\ + 2\,a\,b\,E[(X-\mu_X)(Y-\mu_Y)]\,, \end{aligned} \tag{22}$$

where the terms $E[(X-\mu_X)^2]$ and $E[(Y-\mu_y)^2]$ are the second order moments of the variable X and Y respectively, while the term $E[(X-\mu_X)(Y-\mu_Y)]$ represents the covariance between X and Y. Eq. (22) can thus be re-arranged as:

$$m_2(Z) = a^2\,m_2(X) + b^2\,m_2(Y) + 2\,a\,b\,\mathrm{cov}(X,Y). \tag{23}$$

Eq. (23) states that the second statistical moment of a random variable given by the sum of two random variables, can be determined by considering the individual central moments of each random variable and their covariance. Furthermore, any constant terms can later be included to appropriately scale

the values of the second statistical moments and the covariance. This indicates that the second statistical moment of a generic structural response given by the sum of random variables, as done by the modal equation shown in Eq. (8), can be computed by addressing the second statistical moments of the modal coordinates and their covariance, without the need to directly evaluate the structural response. Further, if random variables X and Y are uncorrelated, the covariance is zero, and Eq. (23) can be further shortened. A similar approach can be used to compute the third-order central moments of the random variable Z:

$$\begin{aligned} m_3(Z) &= E\left[(Z-\mu_Z)^3\right] = E\left[(a\,(X-\mu_x)+b\,(Y-\mu_y))^3\right] \\ &= E\left[a^3\,(X-\mu_X)^3 + b^3\,(Y-\mu_Y)^3\right. \\ &\quad + 3\,a^2\,b\,(X-\mu_X)^2(Y-\mu_Y) \\ &\quad \left. + 3\,a\,b^2\,(X-\mu_X)(Y-\mu_Y)^2\right]. \end{aligned} \tag{24}$$

Also in this case, exploiting the properties of expectation, the constant terms a and b can be moved out from the expectation $E[\cdot]$ and thus (24) can be re-formulated as:

$$\begin{aligned} m_3(Z) = a^3\,E\left[(X-\mu_X)^3\right] &+ b^3\,E\left[(Y-\mu_Y)^3\right] \\ &+ 3\,a^2\,b\,E\left[(X-\mu_X)^2(Y-\mu_Y)\right] \\ &+ 3\,a\,b^2\,E\left[(X-\mu_X)(Y-\mu_Y)^2\right], \end{aligned} \tag{25}$$

where the terms $E\left[(X-\mu_X)^3\right]$ and $E\left[(Y-\mu_Y)^3\right]$ are the third order statistical moments $m_3(X)$ and $m_3(Y)$ of the variable X and Y, respectively. The terms $E\left[(X-\mu_X)^2(Y-\mu_Y)\right]$ and $E\left[(X-\mu_X)(Y-\mu_Y)^2\right]$ are called mixed-terms. They account for the coupling of the random variables and can be denoted as MT_{X^2Y} and MT_{XY^2} respectively. According to this notation, Eq. (25) can be re-arranged as:

$$m_3(Z) = a^3\,m_3(X) + b^3\,m_3(Y) + 3\,a^2\,b\,MT_{X^2Y} + 3ab^2\,MT_{XY^2}\,. \tag{26}$$

Eq. (26) shows that the third central statistical moment of a random variable Z, which is composed of two random variables X and Y, can be obtained by separately considering the third statistical moments of X and Y, along with the mixed terms. These terms do not depend on constant values and

can therefore be computed separately and scaled accordingly.
An identical method can be adopted to compute the fourth-order statistical moment of the variable Z. Indeed, substituting (20) into (2), the fourth order statistical moment can be obtained as:

$$m_4(Z) = E\left[(Z-\mu_Z)^4\right] = E\left[(a\,(X-\mu_X) + b\,(Y-\mu_Y))^4\right]\,. \tag{27}$$

Previous equation can be expanded as:

$$\begin{aligned} m_4(Z) = E\big[&a^4\,(X-\mu_X)^4 + b^4\,(Y-\mu_Y)^4 \\ &+ 4\,a^3\,b\,(X-\mu_X)^3(Y-\mu_Y) \\ &+ 4\,a\,b^3\,(X-\mu_X)(Y-\mu_Y)^3 \\ &+ 6\,a^2\,b^2\,(X-\mu_X)^2(Y-\mu_Y)^2\,. \end{aligned} \tag{28}$$

According to the linearity properties, the expectation can be computed separately for each variable and the constant terms can be moved out from the expected value operator $E[\cdot]$. Eq. (28) thus becomes:

$$\begin{aligned} m_4(Z) = a^4\,E\left[(X-\mu_X)^4\right] &+ b^4\,E\left[(Y-\mu_Y)^4\right] \\ &+ 4\,a^3\,b\,E\left[(X-\mu_X)^3(Y-\mu_Y)\right] \\ &+ 4\,a\,b^3\,E\left[(X-\mu_X)(Y-\mu_Y)^3\right] \\ &+ 6\,a^2\,b^2\,E\left[(X-\mu_X)^2(Y-\mu_Y)^2\right]\,, \end{aligned} \tag{29}$$

where the terms $a^4\,E\left[(X-\mu_X)^4\right]$ and $b^4\,E\left[b(Y-\mu_Y)^4\right]$ are the fourth order central moments $m_4(X)$ and $m_4(Y)$ of variables X and Y respectively. The other terms are still mixed-terms and account for the coupling between variables. In order, such mixed-terms can be denoted as MT_{X^3Y}, MT_{XY^3} and $MT_{X^2Y^2}$. According to this notation, Eq. (29) can be re-written as:

$$\begin{aligned} m_4(Z) = a^4\,m_4(X) &+ b^4\,m_4(Y) \\ &+ 4\,a^3\,b\,MT_{X^3Y} + 4\,a\,b^3\,MT_{XY^3} \\ &+ 6\,a^2\,b^2\,MT_{X^2Y^2}\,. \end{aligned} \tag{30}$$

Eq. (30) demonstrates that the fourth-order statistical moment of a random variable Z defined as the sum of random variables, can be computed by separately evaluating the central moments of each variable and the mixed

terms. Again, central moments and mixed-terms do not depend on any multiplying constants and can thus be scaled later.
It is worth highlighting that, for uncorrelated random variables, the covariance and mixed terms are zero, and Eqs. (23), (26), and (30) can be further simplified. However, in real structures, vibrating modes are generally coupled, meaning the covariance between modal coordinates is not zero. Therefore, omitting the covariance and mixed terms in Eqs. (23), (26), and (30) leads to approximated results. For this reason, the complete equations for calculating central moments will be used throughout the manuscript. The approach herein introduced allows for obtaining the statistical moments of a random variable given by the sum of two random variables.

Generalization to multiple degree of freedom systems. Since Eq. (20) can represent the modal response of a two-degree-freedom system, what is seen until now can be expanded to the modal response of a multi-degree-freedom system (mdof), as a finite element model.
When dealing with fatigue application, what deserves to be computed is the stress time history for each element of an FE model. Assuming a uniaxial stress state, the stress time history of the rth element of the model can be obtained via the modal approach, as shown in Eq. (8), as follows:

$$\sigma(t) = \sum_{i=1}^{n} \phi_{i,\sigma} \cdot q_i(t) = \phi_{1,\sigma}\, q_1 + ... + \phi_{n,\sigma}\, q_n\,. \tag{31}$$

In Eq. (31), $q_i(t)$ are the modal coordinates, $\phi_{i,\sigma}$ are the modal shapes of one stress component. n represents the number of considered vibrating modes. In Eq. 31, modal coordinates $q_i(t)$ are random variables while modal shapes $\phi_{i,\sigma}$ can be considered as constant terms. For this reason, to obtain the second statistical moment of the structural response $\sigma(t)$, Eq. (31) must be substituted into Eq. (2). Grouping similar terms one obtains:

$$m_2(\sigma(t)) = E[(\phi_{1,\sigma}\,(q_1 - \mu_{q_1}) + \phi_{2,\sigma}\,(q_2 - \mu_{q_2}) + ... + \phi_{n,\sigma}\,(q_n - \mu_{q_n}))^2]\,. \tag{32}$$

By solving the square of the polynomial, and exploiting the linearity properties of expected values, Eq. (32) becomes:

$$
\begin{aligned}
m_2(\sigma(t)) = {} & \phi_{1,\sigma}^2\, E[(q_1 - \mu_{q_1})^2] + \phi_{2,\sigma}^2\, E[(q_2 - \mu_{q_2})^2] + \\
& ... + \phi_{n,\sigma}^2\, E[(q_n - \mu_{q_n})^2] + 2\phi_{1,\sigma}\, \phi_{2,\sigma}\, E[(q_1 - \mu_{q_1})(q_2 - \mu_{q_2})] + \\
& ... + 2\phi_{1,\sigma}\, \phi_{n,\sigma}\, E[(q_1 - \mu_{q_1})(q_n - \mu_{q_n})] + \\
& + 2\phi_{2,\sigma}\, \phi_{n,\sigma}\, E[(q_2 - \mu_{q_2})(q_n - \mu_{q_n})]\,.
\end{aligned} \tag{33}
$$

The first three expected value $E[\cdot]$ terms in Eq. (33) are the second statistical moment of modal coordinates, while the last three expected value $E[\cdot]$ represent the covariance between the modal coordinates. Eq. (33) can thus be re-written in a compact form as:

$$
m_2(\sigma(t)) = \sum_{i=1}^{n} (\phi_{i,\sigma})^2\, m_2(q_i) + 2 \sum_{i=1}^{n} \sum_{j=i+1}^{n} \phi_{i,\sigma}\, \phi_{j,\sigma}\, \mathrm{cov}(q_i, q_j)\,. \tag{34}
$$

The second order statistical moment of the modal coordinates $m_2(q_i)$ and the covariance $cov(q_i, q_j)$ between modal coordinates are independent by the modal shapes $\phi_{i,\sigma}$ and $\phi_{j,\sigma}$ and thus can be computed only once and stored into a variable. This means that the second-order statistical moment of the stress response of each element can be computed only by multiplying the second-order statistical moments of the modal coordinates $m_2(q_i)$ and the covariance $\mathrm{cov}(q_i, q_j)$ with the modal shapes $\phi_{i,\sigma}$ and $\phi_{j,\sigma}$. This avoids evaluating the physical response of each element from which to compute the statistical descriptors. This results in computationally efficient.
A similar procedure can be adopted also for higher-order moments. The third-order central moment of the stress response relative to the r^{th} element model, can be obtained by the modal response as:

$$
\begin{aligned}
m_3(\sigma(t)) = {} & \sum_{i=1}^{n} (\phi_{i,\sigma})^3\, m_3(q_i) + \\
& + 3 \sum_{i=1}^{n} \sum_{\substack{j=1 \\ i \neq j}}^{n} \phi_{i,\sigma}^2\, \phi_{j,\sigma}\, E\left[(q_i - \mu_{q_i})^2 (q_j - \mu_{q_j})\right] + \\
& + 6 \sum_{i=1}^{n} \sum_{j=i+1}^{n} \sum_{k=j+1}^{n} \phi_{i,\sigma}\, \phi_{j,\sigma}\, \phi_{k,\sigma}\, E\left[(q_i - \mu_{q_i})(q_j - \mu_{q_j})(q_k - \mu_{q_k})\right]\,.
\end{aligned} \tag{35}
$$

The fourth-order statistical moments of the stress response $\sigma(t)$ can be obtained via the modal approach with an identical pathway as for the other statistical moments. The fourth order statistical moment $m_4(\sigma(t))$ takes the form:

$$
\begin{aligned}
m_4(\sigma(t)) = & \sum_{i=1}^{n} (\phi_{i,\sigma})^4 \, m_4(q_i) \\
& + 4 \sum_{i=1}^{n} \sum_{\substack{j=1 \\ i \neq j}}^{n} (\phi_{i,\sigma})^3 \, \phi_{j,\sigma} \, E[(q_i - \mu_{q_i})^3 (q_j - \mu_{q_j})] \\
& + 6 \sum_{i=1}^{n} \sum_{\substack{j=1 \\ i \neq j}}^{n} (\phi_{i,\sigma})^2 \, (\phi_{j,\sigma})^2 \, E[(q_i - \mu_{q_i})^2 (q_j - \mu_{q_j})^2] \\
& + 12 \sum_{i=1}^{n} \sum_{j=1}^{n} \sum_{\substack{k=1 \\ i \neq j,k \\ j \neq k}}^{n} (\phi_{i,\sigma})^2 \, \phi_{j,\sigma} \, \phi_{k,\sigma} \, E[(q_i - \mu_{q_i})^2 (q_j - \mu_{q_j})(q_k - \mu_{q_k})] \\
& + 24 \sum_{i=1}^{n} \sum_{j=1}^{n} \sum_{k=1}^{n} \sum_{\substack{l=1 \\ i \neq j,k,l \\ j \neq k,l \\ k \neq l}}^{n} \phi_{i,\sigma} \, \phi_{j,\sigma} \, \phi_{k,\sigma} \, \phi_{l,\sigma} \, E[(q_i - \mu_{q_i})(q_j - \mu_{q_j})(q_k - \mu_{q_k})(q_l - \mu_{q_l})] \, .
\end{aligned}
\tag{36}
$$

In Eq. (35) and in Eq. (36), $m_3(q_i)$ and $m_4(q_i)$ are the third-order and the fourth-order statistical moments of modal coordinates respectively. All the expectation $E[\cdot]$ are instead mixed terms that account for the coupling of vibrating modes. Also, in this case, the statistical moments of modal coordinates and mixed terms are independent of the scaling modal shapes and thus can be computed once and stored into variables. To obtain the statistical moments of the stress response of each element of the model $\sigma(t)$, necessary to compute the kurtosis and skewness, is then possible to combine these variables with the element modal shapes. Eq. (35) and (36) take into account all the possible permutations and thus are valid for whichever number of vibrating modes. It is worth renewing that in case the modal coordinates are uncorrelated, then the covariance is zero, and Eqs. (34), (35) and (36) could be further simplified. However, even if modal coordinates are weakly coupled, omitting the covariance and the mixed terms may lead to

incorrect results.
Eqs. (34), (35) and (36) have shown that the central moments, as well as the higher-order statistical descriptors such as kurtosis and skewness, of the structural response, can be computed by exploiting the modal approach without the need to evaluate the structural response of each element. It is important to note that the proposed approach allows for the evaluation of central moments of physical quantities, such as the stress components, individually. At present, the proposed approach does not include a multiaxial synthesis. However, in the case of the uniaxial stress condition, the evaluation of the correction coefficient, which accounts for the non-Gaussianity of the stress response, can be shortened as shown in Fig. 1.

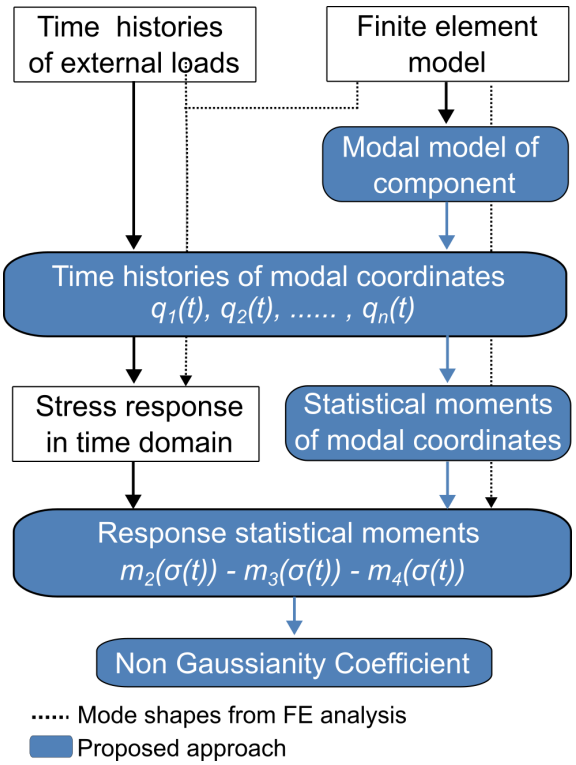

Figure 1: Flowchart of the procedure idealized to quickly calculate the central moments of a structural response by modal approach

4. Synthetic experiment

To evaluate the accuracy of the proposed approach in computing the central moments of the structural response of a vibrating system exploiting the modal approach, the FE model shown in Fig. 2 is used as a test case.

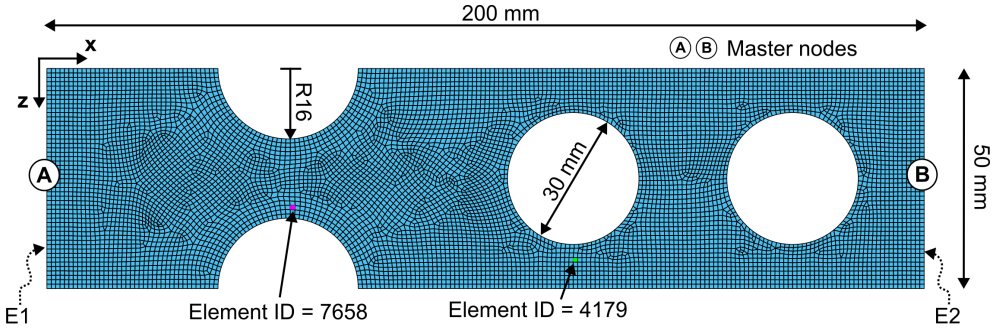

Figure 2: Finite element model used as test-case.

The model is composed of 7997 shell elements with a constant thickness of 0.5 mm. An element size of 1mm was used for the mesh. This, besides the use of four-node shell elements with six degree of freedom at each node, ensures a good approximation of the structural response while maintaining reasonable computational efficiency. A mesh sensitivity analysis was not necessary for the scope of the paper. Indeed, even if the results may slightly vary according to mesh size, the accuracy of the proposed method relative to the standard approach would not be compromised since the comparison is referred to the same FE model. The model is realized with structural steel considering a Young modulus equal to $2{\cdot}10^{11}$ Pa, a Poisson modulus ν=0.3 and a density equal to $\rho = 7850$ Kg/m^3. Being in the region of high-cycle fatigue, a linear elastic material model was adopted, and the plasticity of the material was not considered. As shown in Fig. 2, the nodes on the edges E1 and E2 are respectively constrained to master nodes A and B respectively (Fig. 2) by RBE2 (Rigid Body Element) elements. The master nodes A and B shown in Fig. 2 were meshed as mass elements with a mass equal to 1000 Kg. This allows for using the large-mass method approach to excite the structures with two uncorrelated excitations [41]. To excite the structures in the y-direction (out of plane) according to the reference system shown in Fig. 2, the two master nodes were rigidly constrained to the ground leaving free the displacements in the y-direction, and the rotations around the

z-direction.
To define the frequency range of the excitation PSD and to obtain the necessary information to realize the dynamic model, a modal analysis, has been performed and the first 5 vibrating modes were extracted. The obtained natural frequencies are $f_1 = 25.6$ Hz, $f_2 = 103.5$ Hz, $f_3 = 160.7$ Hz, $f_4 = 237.8$ Hz and $f_5 = 383.8$ Hz respectively. According to the obtained natural frequencies, an uncorrelated excitation PSD matrix (off-diagonal terms equal to zero) of dimension $[2 \times 2 \times 200000]$ was generated, where the terms on the main diagonal are identical. The PSD profile is shown in Fig. 3a.

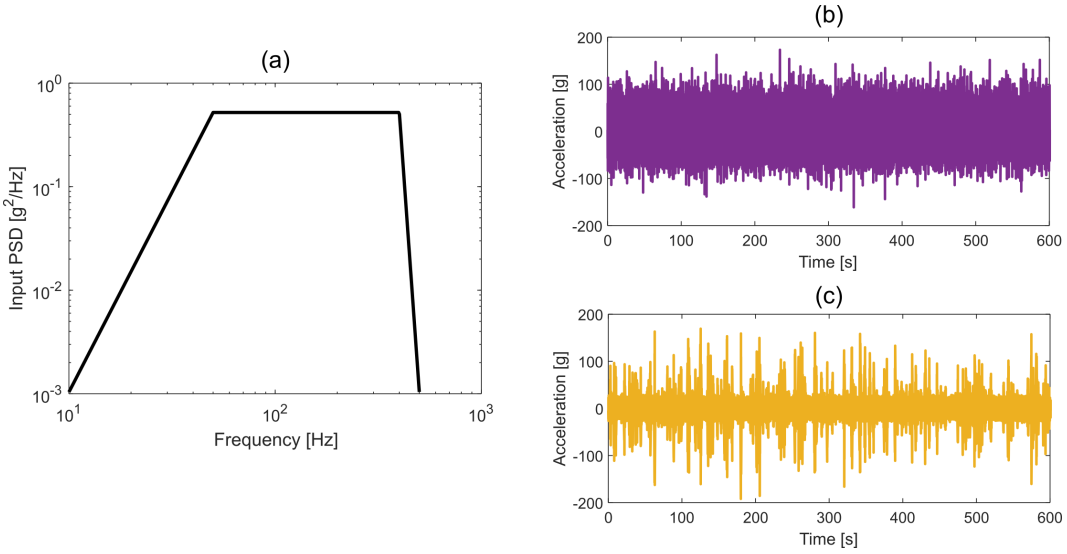

Figure 3: Load excitation used to test the proposed method: (a) Excitation PSD, (b) Stationary non-Gaussian signal, (c) Non-stationary non-Gaussian signal.

From the excitation PSD matrix, two random signals were generated and used as input for the dynamic model. A frequency sampling of 40000 Hz was used to accurately capture the dynamic behavior of the structure. The generated signals are shown in Figs. 3b and 3c, respectively. The signal shown in Fig. 3b is a stationary, non-Gaussian signal generated using the approach implemented in WAFO [42]. It has a kurtosis value of 7.32 and a skewness of 0.41. On the other hand, the signal shown in Fig. 3c is a non-stationary, non-Gaussian signal generated with the carrier-wave approach introduced by Kihm [23]. It has a kurtosis value of 11.52 and a skewness of zero. Since in this manuscript, the central moments are evaluated on

the entire time series, the use of non-stationary excitation was not strictly necessary. According to the results of Palmieri et al. [12], Khim et al. [23], Sgamma et al. [24], and Braccesi et al. [25], the use of non-stationary non-Gaussian signals was only used to induce a non-Gaussian response of the structure.

From the modal analysis, the natural frequencies and displacement modal shapes were extracted to build a dynamic model. A constant damping ratio of 3% was used for all vibrating modes. The physical quantity used in this paper to evaluate the accuracy of the proposed approach in estimating the central moment, exploiting the modal approach, is the normal stress in the x-direction according to the reference system shown in Fig. 2. The PSD of normal stress in the x-direction for element ID 7658 and element ID 4179 (identified in Fig. 2) are shown in Fig. 4.

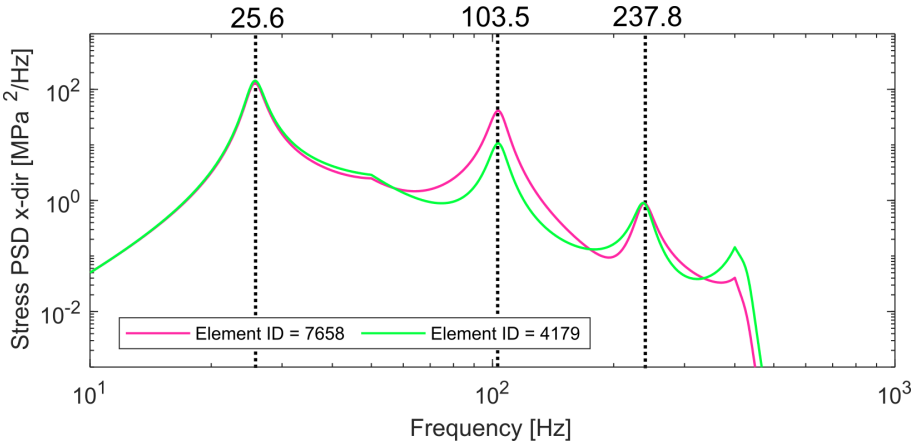

Figure 4: PSD of normal stress in x-direction for element ID 7658 and element ID = 4179.

As visible from Fig. 4, the response stress PSD is characterized by two main vibrating modes, at 25.6 Hz and 103.6 Hz respectively. Another non-negligible vibrating mode is at 237.8 Hz. The obtained PSD shown in Fig. 4 is close to that of real structures.

The procedure presented in Sec. 3 is applied to the proposed structures to evaluate the central moments m_2, m_3 and m_4 and the higher-order moments (kurtosis and skewness) for all the 7997 elements. To this aim, despite the response PSD is mainly affected by the first two vibrating modes, due to the generality of the proposed method, all the first five extracted vibrating

modes were considered. To evaluate the accuracy of the results obtained with the proposed approach, the central moments from the second up to the fourth order were computed also with the standard approach evaluating the structural response (normal stress in the x-direction) for all elements. The comparison between the standard and the proposed approach is shown in Fig. 5 where the second, third, and fourth-order central moments color maps are compared. On the left side of Fig. 5 the results obtained with the standard procedure while on the right side of Fig. 5 the results obtained with the proposed approach.

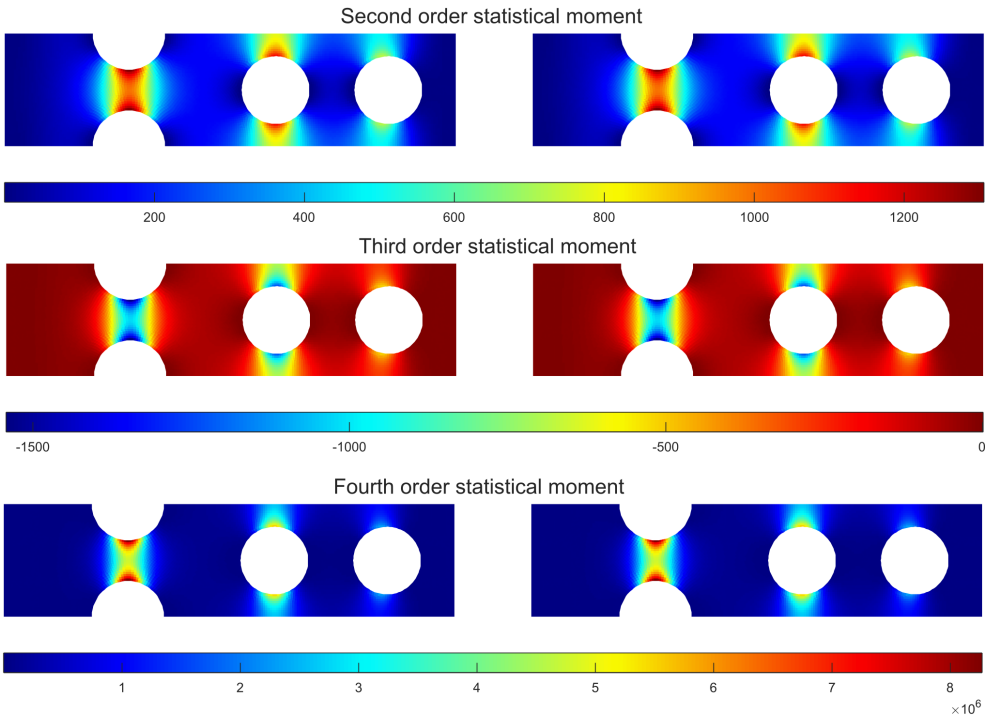

Figure 5: Comparison between color maps for the second, third, and fourth-order central moments obtained with the classical approach (left) and the proposed procedure (right).

As visible from Fig. 5, the results obtained with the proposed approach compared to that derived by the classical procedure are identical and no differences appear. Once the central moments are available, high-order central moments (kurtosis and skewness) can be obtained by Eq. (3). The resulting kurtosis and skewness, obtained with the proposed approach are

shown in Fig. 6 and in Fig. 7 respectively. Identical results are obtained with the standard approach. Indeed, if the modal decomposition is retained valid, then the proposed method for the identification of central moments is a closed-form solution.

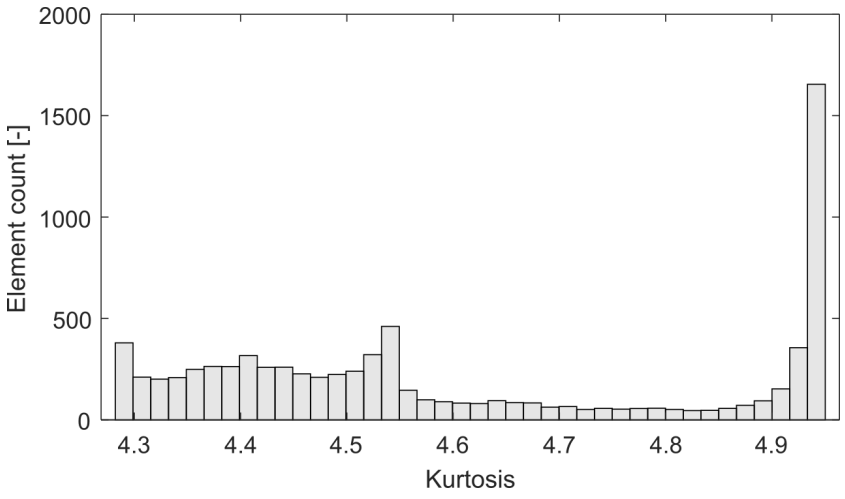

Figure 6: Histogram of obtained kurtosis with the proposed approach. Identical results are obtained with the standard approach.

An important difference is in the computational time necessary to obtain the kurtosis and skewness for all elements. The calculation of the central moments with the standard approach for all the 7997 elements is equal to 6423.0s, while with the proposed approach the needed computational time is equal to 18.52s, thus showing a reduction of around two orders of magnitude (Further details about computational time are given in Appendix A). This indicates that the computational advantage, when dealing with a large FE model consisting of millions of elements (which is typical in industrial applications), becomes considerable. All the calculations were performed with a computer with processor i9-9900K CPU @3.60GHz and 64 GB of RAM. Moreover, the correction factor is computed for each element of the model with the exact value of kurtosis and skewness thus avoiding assumptions that may affect the results. It is worth noting that, despite in this activity only the central moments of normal stress in the x-direction are computed, the proposed approach applies to any physical quantities of interest (*i.g.* displacement, acceleration, deformation, etc) without limitations. The central

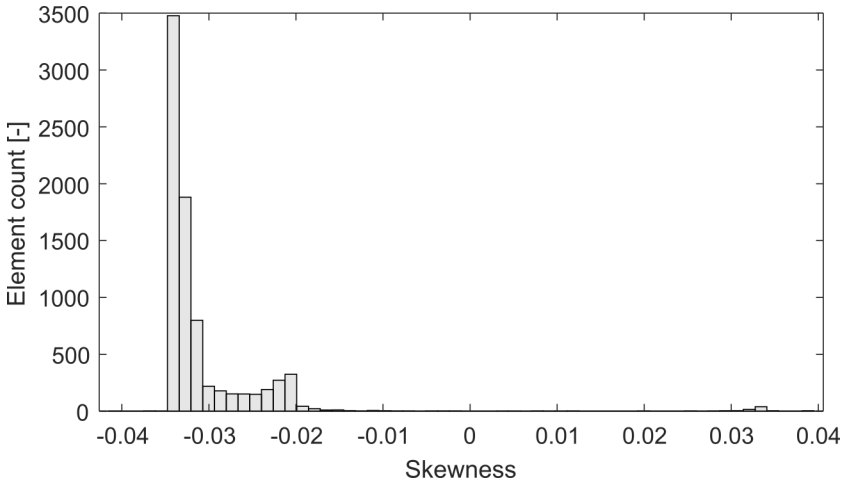

Figure 7: Histogram of obtained skewness with the proposed approach. Identical results are obtained with the standard approach.

moments of the stress response are considered in this work simply because, for the evaluation of fatigue damage, it is the most relevant physical quantity.

5. Conclusion

Calculating fatigue damage for structures subjected to non-Gaussian random vibrations is a challenging task when using traditional spectral methods, developed for high-cycle fatigue conditions as these methods do not account for the non-Gaussian characteristics of the loads. In engineering practice, correction coefficient methods are employed to improve accuracy; however, they rely on the kurtosis and skewness of the structural response, typically requiring time-domain analysis and thereby reducing the computational efficiency advantages of spectral methods.

In this research, a novel method for the fast estimation of central moments was introduced. The method is based on a modal approach commonly used in structural dynamics. It was shown that when the structural response is expressed as a linear combination of modal coordinates, the central moments of these coordinates can be directly evaluated. The proposed method's primary step involves calculating the central moments of the modal coordinates and their mixed terms, which account for interactions between vibrating modes. Once these central moments and mixed terms are known, the physical central

moments—such as kurtosis and skewness—of a generic structural response (e.g., stress or strain) can be directly determined through a straightforward combination with the modal shapes. This approach enables significant computational time saving by eliminating the need for time-domain simulations to evaluate the structural response. This time saving is achieved because, exploiting the modal approach, the central moments and mixed terms are calculated solely for the chosen set of modal coordinates, rather than for the full set of system degrees of freedom.
The introduced method was validated by synthetic experiment, and it was confirmed that the results were identical to those obtained through classical procedure. The findings of this paper demonstrate that spectral methods, in conjunction with correction coefficient approaches, may be effectively applied even in scenarios involving non-Gaussian loads, while maintaining the computational efficiency typical of spectral methods. The proposed procedure, however, allows for the fast calculation of the central moments of the individual components of the stress tensor. Consequently, in the framework of vibration fatigue, it is applicable only when one stress component predominates over the others. It will therefore be necessary to further develop the proposed method to combine the central moments of the stress components according to a multiaxial synthesis criterion. In this way, the applicability of the proposed procedure can be extended to any stress condition (uniaxial or multiaxial).

Acknowledgments

The authors acknowledge partial financial support from the Slovenian Research Agency (research core funding No. P2-0263).

Authors Contributions: All authors contributed equally.
Conflicts of Interest: The authors declare no conflict of interest.

References

[1] ASTM-E1049-85, Standard practices for cycle counting in fatigue analysis (Reapproved 2011).

[2] M. Muñiz-Calvente, A. Álvarez Vázquez, F. Pelayo, M. Aenlle, N. García-Fernández, M. Lamela-Rey, A comparative review of time-

and frequency-domain methods for fatigue damage assessment, International Journal of Fatigue 163 (2022) 107069.

[3] A. Zorman, J. Slavič, M. Boltežar, Vibration fatigue by spectral methods—a review with open-source support, Mechanical Systems and Signal Processing 190 (2023) 110149.

[4] M. Palmieri, F. Cianetti, G. Zucca, G. Morettini, C. Braccesi, Spectral analysis of sine-sweep vibration: A fatigue damage estimation method, Mechanical Systems and Signal Processing 157 (2021).

[5] G. Zucca, M. Palmieri, F. Cianetti, On the statistical distribution of the maxima of sine on random process, Mechanical Systems and Signal Processing 158 (2021).

[6] J. Slavič, M. Boltezar, M. Mrsnik, M. Cesnik, J. Javh, Vibration Fatigue by Spectral Methods. From Structural Dynamics to Fatigue Damage – Theory and Experiments, Elsevier, 1st edition, 2020.

[7] D. E. Newland, An Introduction to Random Vibrations, Spectral and Wavelet Analysis, Courier Corporation, 2012.

[8] F. Xu, H. Yang, K. Ahlin, On vehicle response under non-gaussian road profile excitation, Advances in Mechanical Engineering 16 (2024) 16878132241241676.

[9] J. Ding, X. Chen, Fatigue damage evaluation of broad-band gaussian and non-gaussian wind load effects by a spectral method, Probabilistic Engineering Mechanics 41 (2015) 139 – 154.

[10] M. K. Ochi, Non-gaussian random processes in ocean engineering, Probabilistic Engineering Mechanics 1 (1986) 28–39.

[11] K. Sweitzer, Random vibration response statistics for fatigue analysis of nonlinear structures, Ph.D. thesis, Rochester Institute of Technology, 2006.

[12] M. Palmieri, M. Česnik, J. Slavič, F. Cianetti, M. Boltežar, Non-gaussianity and non-stationarity in vibration fatigue, International Journal of Fatigue 97 (2017) 9 – 19.

[13] A. Niesłony, M. Böhm, T. Łagoda, F. Cianetti, The use of spectral method for fatigue life assessment for non-gaussian random loads, Acta Mechanica et Automatica 10 (2016) 43–50.

[14] M. Wang, C. Wang, Y. Guan, A comparative study on damage analysis between gaussian and non-gaussian random vibration, Vibroengineering PROCEDIA 12 (2017) 72–77.

[15] A. Chang, H. Li, S. Wang, D. Junfeng, Probabilistic analysis and fatigue damage assessment of offshore mooring system due to non-gaussian bimodal tension processes., Journal of Ocean University of China 16 (2017) 585–601.

[16] P. Wolfsteiner, Fatigue assessment of non-stationary random vibrations by using decomposition in gaussian portions, International Journal of Mechanical Sciences 127 (2017) 10–22.

[17] A. Trapp, P. Wolfsteiner, Fatigue assessment of non-stationary random loading in the frequency domain by a quasi-stationary gaussian approximation, International Journal of Fatigue 148 (2021) 106214.

[18] S. R. Winterstein, Nonlinear vibration models for extremes and fatigue, Journal of Engineering Mechanics 114 (1988) 1772 – 1790.

[19] X. Wang, J. Sun, Effect of skewness on fatigue life with mean stress correction, Journal of Sound and Vibration 282 (2005) 1231–1237.

[20] C. Braccesi, F. Cianetti, G. Lori, D. Pioli, The frequency domain approach in virtual fatigue estimation of non-linear systems: The problem of non-gaussian states of stress, International Journal of Fatigue 31 (2009) 766–775.

[21] F. Cianetti, M. Palmieri, C. Braccesi, G. Morettini, Correction formula approach to evaluate fatigue damage induced by non-gaussian stress state, Procedia Structural Integrity 8 (2018) 390 – 398.

[22] K. Yuan, Z. Sun, A spectral method for accurate evaluation of fatigue damage induced by wide-band non-gaussian random processes, Ocean Engineering 281 (2023) 115002.

[23] F. Kihm, S. Rizzi, S. Ferguson, A. Halfpenny, Understanding how kurtosis is transferred from input acceleration to stress response and it's influence on fatigue life.

[24] M. Sgamma, M. Palmieri, M. Barsanti, F. Bucchi, F. Cianetti, F. Frendo, Study of the response of a single-dof dynamic system under stationary non-gaussian random loads aimed at fatigue life assessment, Heliyon 10 (2024).

[25] C. Braccesi, F. Cianetti, M. Palmieri, G. Zucca, The importance of dynamic behaviour of vibrating systems on the response in case of non-gaussian random excitations, Procedia Structural Integrity 12 (2018) 224 – 238.

[26] A. Trapp, F. Hollweck, P. Wolfsteiner, On the transmission of non-gaussian random loading through linear structures, Procedia Structural Integrity 37 (2022) 622–631.

[27] F. Cianetti, Development of a modal approach for the fatigue damage evaluation of mechanical components subjected to random loads, Structural durability and Health monitoring 8 (2012) 1–29.

[28] M. Mršnik, J. Slavič, M. Boltežar, Vibration fatigue using modal decomposition, Mechanical Systems and Signal Processing 98 (2018) 548–556.

[29] N. M. M. Maia, J. M. M. Silva, Theoretical and Experimental Modal Analysis, Research Studies Press, 1997.

[30] C. Braccesi, F. Cianetti, L. Tomassini, Fast evaluation of stress state spectral moments, International Journal of Mechanical Sciences 127 (2017) 4–9.

[31] J. S. Bendat, A. G. Piersol, Random Data: Analysis and Measurement Procedures, John Wiley & Sons, 4th edition, 2010.

[32] A. Preumont, Random Vibration and Spectral Analysis, Springer, 1994.

[33] O. C. Zienkiewicz, R. L. Taylor, J. Z. Zhu, The Finite Element Method: Its Basis and Fundamentals, Sixth Edition, Butterworth-Heinemann, 6 edition, 2005.

[34] A. A. Shabana, Dynamics of Multibody Systems, Cambridge University Press, 2020.

[35] A. Carpinteri, A. Spagnoli, S. Vantadori, A review of multiaxial fatigue criteria for random variable amplitude loads, Fatigue and Fracture of Engineering Material and Structures 40 (2017) 1007–1036.

[36] C. Braccesi, G. Morettini, F. Cianetti, M. Palmieri, Evaluation of fatigue damage with an energy criterion of simple implementation, Procedia Structural Integrity 8 (2017) 192–203.

[37] A. Niesłony, M. Böhm, R. Owsiński, Formulation of multiaxial fatigue failure criteria for spectral method, International Journal of Fatigue 135 (2020).

[38] X. Pitoiset, A. Preumont, Spectral methods for multiaxial random fatigue analysis of metallic structures, International Journal of Fatigue 22 (2000) 541–550.

[39] T. Dirlik, D. Benasciutti, Dirlik and tovo-benasciutti spectral methods in vibration fatigue: A review with a historical perspective, Metals 11 (2021).

[40] F. Cianetti, M. Palmieri, J. Slavič, C. Braccesi, G. Morettini, The effort of the dynamic simulation on the fatigue damage evaluation of flexible mechanical systems loaded by non-gaussian and non stationary loads, International Journal of Fatigue 103 (2017) 60 – 72.

[41] G. de Morais Teixeira, Random vibration fatigue analysis of a notched aluminum beam, International Journal of Mechanical Engineering and Automation 2 (2015).

[42] P. Brodtkorb, P. Johannesson, G. Lindgren, I. Rychlik, J. Rydén, E. Sjö, WAFO - a matlab toolbox for analysis of random waves and loads, 2000.

Appendix A

The computational time required to calculate the central moments using the standard and proposed approach was evaluated by varying the number of samples in the excitation time histories. The frequency sampling rate was kept constant at 40000 Hz, while five different excitation durations — $100s$, $500s$, $600s$, $800s$, $1000s$, and $1500s$ — were considered. Based on these parameters, the corresponding number of samples in the excitation time histories is as follows: $4 \cdot 10^6$ - $2 \cdot 10^7$ - $2.4 \cdot 10^7$ - $3.2 \cdot 10^7$ - $4 \cdot 10^7$ - $6 \cdot 10^7$ respectively. The computational time required to compute the central moments using the standard and proposed approach is summarized in table 1.

Table 1: Comparison between the computational time required to compute the central moments using the standard and proposed approach.

Signal Length $[s]$	Samples $[-]$	Standard approach $[s]$	Proposed approach $[s]$	Ratio $[-]$
100	$4.0 \cdot 10^6$	1116.1	4.37	255.4
500	$2.0 \cdot 10^7$	5373.6	15.63	343.9
600	$2.4 \cdot 10^7$	6423.0	18.52	346.7
800	$3.2 \cdot 10^7$	8521.7	24.28	351.0
1000	$4.0 \cdot 10^7$	10649.4	29.99	355.2
1500	$6.0 \cdot 10^7$	15975.2	44.49	359.1

The ratio in table 1 represents the ratio of the computational time using the standard approach to the computational time using the proposed approach. As observed, the computational time reduction is approximately two orders of magnitude and varies linearly with the number of samples. Figure 8, shows the trend in the computational time for the standard and proposed approach necessary to compute the central statistical moments.

As visible from Fig. 8, the computational time varies linearly for both approaches even if with a different slope.

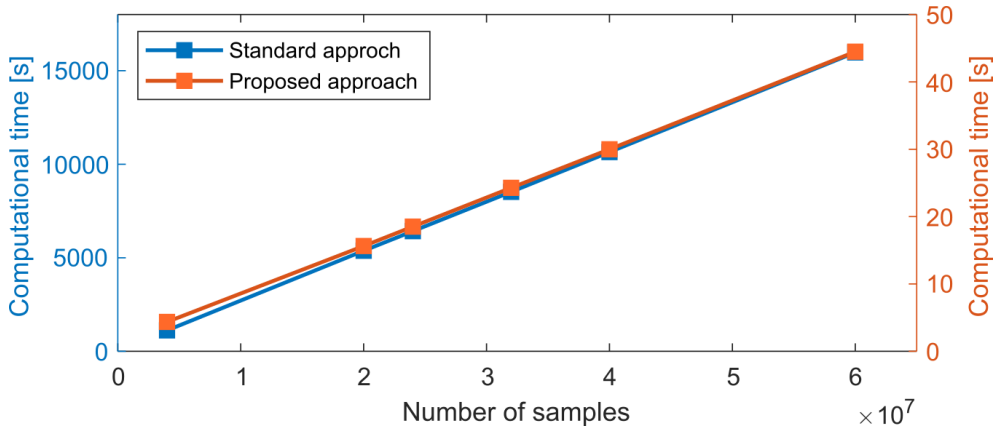

Figure 8: Computational time required to calculate the central moments with the standard and with the proposed approach for different number of samples in the excitation signals.